Scientific Research and Essays Vol. 7(31), pp. 2770-2780, 9 August, 2012
Available online at http://www.academicjournals.org/SRE
DOI: 10.5897/SRE11.576
ISSN 1992-2248 ©2012 Academic Journals

Full Length Research Paper

On spectral-homotopy analysis solutions of steady magnetohydrodynamic (MHD) flow and heat transfer from a rotating disk in a porous medium

A. A. Khidir and P. Sibanda*

School of Mathematics, Statistics and Computer Science, University of KwaZulu-Natal, Private Bag X01 Scottsville 3209, Pietermaritzburg, South Africa.

Accepted 20 June, 2012

In this paper, a new computational technique was used to solve a system of nonlinear second order equations that govern the steady magnetohydrodynamic (MHD) flow of a viscous incompressible and electrically conducting fluid past a rotating disk in a porous medium. Approximate analytic solutions are found and the effects of ohmic heating and viscous dissipation on the fluid properties are determined. The results are presented graphically.

Key words: Magnetohydrodynamic (MHD) flow, heat transfer, rotating disk, porous medium, Chebyshev spectral method, spectral-homotopy analysis method.

INTRODUCTION

The pioneering study of fluid flow due to a rotating disk in a fluid of infinite extent was carried out by von Karman (1921) who introduced transformations that reduced the governing partial differential equations to ordinary differential equations. Follow up studies were made by Cochran (1934) who improved von Karman's results by using a Taylor series expansion near the disk and a series solution involving exponentially decaying functions far from the disk and by Benton (1966) who solved the unsteady problem.

In the last few decades, studies by Attia (2004, 2006, 2007) considered the effects of (1) ion slip (2) temperature depend viscosity, and (3) ohmic heating on rotating disk flow. Chen (2004) investigated the effects of ohmic and viscous heating, while Eldabe and Ouaf (2006) presented a study of the rotating disk problem with heat and mass transfer in an incompressible, magneto-micropolar fluid flow with ohmic heating, and viscous dissipation. They indicated that an increase in the magnetic parameter gives a decrease in the values of the velocity, Nusselt and Sherwood numbers. Other recent studies of the rotating disk flow that provide a suitable framework for this work include those by Osalusi and Sibanda (2006) who considered variable property laminar convective flow due to a porous disk and Frusteri and Osalusi (2007) who considered ion slip effects and variable fluid properties. Osalusi et al. (2007, 2008) considered, respectively ohmic heating and viscous dissipation for flow over a porous rotating disk and the combined effects of viscous dissipation and Joule heating on unsteady hydromagnetic flow of a viscous fluid on a rotating cone in a rotating fluid in the presence of Hall and ion-slip currents taking into account the variable properties of the fluid. Sahoo (2009) studied the effects of partial slip, viscous dissipation and Joule heating on Von Karman flow and heat transfer of an electrically conducting non-Newtonian fluid.

Turkyilmazoglu (2009) extended the classical von Karman problem of flow over a rotating disk to account for the compressibility effects with insulated and isothermal wall conditions. Turkyilmazoglu (2010) used an exponentially decaying series method to find the solution of the steady laminar flow of an incompressible viscous electrically conducting fluid over a rotating disk in the presence of a uniform transverse magnetic field, while Sibanda and Makinde (2010) studied ohmic

*Corresponding author. E-mail: sibandap@ukzn.ac.za.

heating, viscous dissipation, Hall current and ion slip currents in magnetohydrodynamic (MHD) flow over a porous rotating disk.

A wide variety of problems in science and engineering can be modeled using coupled systems of differential equations. Finding analytical solutions of these systems of nonlinear equations on finite or semi-infinite domains is one of the most challenging problems in nonlinear mechanics. The importance of analytical solutions also lies in their use in the validation of new numerical and perturbation techniques. In recent years, homotopy analysis method has become a popular method for finding semi-analytical solutions of nonlinear differential equations. Xu and Liao (2006) used the homotopy analysis method to find series solutions of unsteady flows of a viscous incompressible electrically conducting fluid caused by an impulsively rotating infinite disk. Dinarvand et al. (2010) employed the homotopy analysis method to study the unsteady laminar incompressible boundary layer flow of a viscous electrically conducting fluid at the stagnation point region of an impulsively rotating and translating sphere with a magnetic field and a buoyancy force. Rashidi and Dinarvand (2009) used the homotopy analysis method for finding the totally analytic solutions of the system of nonlinear ordinary differential equations derived from similarity transform for the steady three-dimensional problem of fluid deposition on an inclined rotating disk. They showed that homotopy analysis method (HAM) is valid for both weakly and strongly nonlinear problems.

The extended homotopy perturbation method (HPM) was used by Ariel (2009) to find analytical solutions of the rotating disk problem. He showed that the extended HPM is highly accurate and the solution converges rapidly to the true solution. However, as pointed out by Liao (2005) and others, the homotopy perturbation method is only a special case of homotopy analysis method, valid when the auxiliary parameter $\hbar = -1$. Recent studies by Motsa et al. (2010a, b) have however cast the spotlight on the limitations of the homotopy analysis method. They suggested a modification that combines the proven strengths of the HAM with the Chebyshev spectral method. It has been claimed that this modification produces an algorithm that has none of the restrictive assumptions associated with the HAM (such as the requirement that the solution sought ought to conform to the so-called rule of solution expression and the rule of coefficient ergodicity), is computationally efficient, converges faster, and is more accurate than the homotopy analysis method.

SPECTRAL-HOMOTOPY ANALYSIS METHOD

The spectral-homotopy analysis method (Motsa et al., 2010a, b; Sibanda et al., 2012), seeks to remove some restrictive assumptions associated with the standard homotopy analysis method. In this method, the selected linear operator is defined in terms of the Chebyshev spectral differentiation matrix. Using this method, any selected initial guess may be used as long as it satisfies the boundary conditions. In the standard HAM, one is restricted to choosing a simple initial guess and linear operator so that the solution of higher order deformation equations is possible.

In this study, we use SHAM to solve coupled nonlinear partial differential equations that describe the motion of an electrically conducting fluid past a rotating porous disk. The present study incorporates the effects of ohmic heating and viscous heat dissipation, Hall currents and an applied magnetic field on a rotating disk flow with constant properties. We test the accuracy, computational efficiency, and robustness of this method by comparing the present results with the numerical results in the literature.

GOVERNING EQUATIONS

We consider the flow due to a rotating disk in a viscous incompressible electrically conducting Newtonian fluid in a porous medium. We consider non-rotating cylindrical polar coordinates (r, φ, z) where z is the vertical axis with r and φ as the radial and tangential axes, respectively. The disk rotates with constant angular velocity Ω about the z-axis in a viscous incompressible electrically conducting Newtonian fluid in a porous medium. The components of the flow velocity are u, v and w in the directions of increasing r, φ and z, respectively. An external uniform magnetic field with constant flux density B_0 is applied perpendicular to the surface of the disk. The induced magnetic field is assumed to be small in comparison with the applied magnetic field. The surface of rotating disk is maintained at a uniform temperature T_w while the temperature of the fluid is T_∞. Under the Boussinesq approximation, the basic equations governing the flow of the fluid in the presence of the porous medium and the energy equation describing the temperature distribution are (Sibanda and Makinde, 2010):

$$\frac{\partial u}{\partial r} + \frac{u}{r} + \frac{\partial w}{\partial z} = 0, \tag{1}$$

$$u\frac{\partial u}{\partial r} + w\frac{\partial u}{\partial z} - \frac{v^2}{r} + \frac{\nu}{k}u = -\frac{1}{\rho}\frac{\partial p}{\partial r} + \nu\left(\frac{\partial^2 u}{\partial r^2} + \frac{1}{r}\frac{\partial u}{\partial r} - \frac{u}{r^2} + \frac{\partial^2 u}{\partial z^2}\right) - \frac{\sigma B_0^2}{\rho(1+s^2)}(u - sv), \tag{2}$$

$$u\frac{\partial v}{\partial r} + \frac{uv}{r} + w\frac{\partial v}{\partial z} + \frac{\nu}{k}v = \nu\left(\frac{\partial^2 v}{\partial r^2} + \frac{1}{r}\frac{\partial v}{\partial r} - \frac{v}{r^2} + \frac{\partial^2 v}{\partial z^2}\right) - \frac{\sigma B_0^2}{\rho(1+s^2)}(v + su), \tag{3}$$

$$u\frac{\partial w}{\partial r} + w\frac{\partial w}{\partial z} + \frac{\nu}{k}v = -\frac{1}{\rho}\frac{\partial p}{\partial z} + \nu\left(\frac{\partial^2 w}{\partial r^2} + \frac{1}{r}\frac{\partial w}{\partial r} + \frac{\partial^2 w}{\partial z^2}\right) + g\beta(T - T_\infty) \tag{4}$$

$$u\frac{\partial T}{\partial r}+w\frac{\partial T}{\partial z}=\frac{\kappa}{\rho C_p}\left(\frac{\partial^2 T}{\partial r^2}+\frac{1}{r}\frac{\partial T}{\partial r}+\frac{\partial^2 T}{\partial z^2}\right)+\frac{2\nu}{C_p}\left(\left[\frac{\partial u}{\partial r}\right]^2+\left[\frac{u}{r}\right]+\left[\frac{\partial w}{\partial z}\right]^2\right)$$

$$+\frac{\nu}{C_p}\left(\left[\frac{\partial v}{\partial z}\right]^2+\left[\frac{\partial w}{\partial r}+\frac{\partial u}{\partial z}\right]^2+\left[r\frac{\partial}{\partial r}\left(\frac{v}{r}\right)\right]^2\right)+\frac{\sigma B_0^2}{\rho C_p}(u^2+v^2), \quad (5)$$

where p is the pressure, ρ is the density of the fluid, ν is the kinematic viscosity of the fluid, T is the fluid temperature, C_p is the specific heat at constant pressure, s is the Hall current, κ is the thermal conductivity of the fluid, and k is the Darcy permeability parameter.

The appropriate boundary conditions of the aforementioned system are:

$$\left.\begin{array}{l} z=0: u=0, w=W,\ v=r\Omega,\ T=T_\infty, \\ z\to\infty: u,v\to 0,\ T\to T_\infty,\ p\to p_\infty \end{array}\right\} \quad (6)$$

where the subscript "∞" denotes ambient conditions. Following Sibanda and Makinde (2010), we introduce the von Karman similarity variable $\eta=(\Omega/\nu)^{1/2}z$ and transformations:

$$F=\frac{u}{r\Omega},\ G=\frac{v}{r\Omega},\ H=\frac{w}{\sqrt{\nu\Omega}},\ \theta=\frac{T-T_\infty}{T_w-T_\infty}\quad\text{and}\quad P=\frac{p-p_\infty}{\rho\nu\Omega}, \quad (7)$$

where η is a non-dimensional distance along the axis of rotation, F, G, and H are the non-dimensional radial, tangential, and axial velocities, and θ is the temperature. Using the aforementioned transformations, Equations 1 to 5 reduce to the second order nonlinear differential equations:

$$F''-HF'-F^2+G^2-Da^{-1}F-\frac{M}{1+s^2}(F-sG)=0, \quad (8)$$

$$H''-HH'-Da^{-1}H+Gr\,\theta=0, \quad (9)$$

$$G''-HG'-2FG-Da^{-1}G-\frac{M}{1+s^2}(G+sF)=0, \quad (10)$$

$$\frac{1}{Pr}\theta''-H\theta'+\frac{2Ec}{Re}\left[(H')^2+2F^2\right]+Ec\left[(G')^2+(F')^2\right]+MEc(F^2+G^2)=0. \quad (11)$$

The physical parameters appearing in Equations 8 to 11 are:

$$Da=\frac{k\Omega}{\nu},\ M=\frac{\sigma B_0^2}{\rho\Omega},\ Gr=\frac{g\beta(T_w-T_\infty)}{\sqrt{\nu\Omega^3}},\ Ec=\frac{r^2\Omega^2}{C_p\Delta T},\ Re=\frac{r^2\Omega}{\nu} \quad (12)$$

where Da is the local Darcy number, M is the magnetic interaction parameter, Gr is the modified Grashof number, Pr is Prandtl number, Re is the Reynolds number, and Ec is the Eckert number.

The primes in Equations 8 to 11 denote differentiation with respect to η. The system of the aforementioned equations are solved subject to the boundary conditions:

$$\left.\begin{array}{ll} F=0, H=H_w, G=\theta=1 & \text{at}\quad \eta=0 \\ F=G=H=\theta=0 & \text{as}\quad \eta\to\infty \end{array}\right\} \quad (13)$$

where $H_w=W/\sqrt{\nu\Omega}$ is the suction ($H_w<0$) or injection ($H_w>0$) velocity at the disk surface. In this study, we use the spectral-homotopy analysis method to find the solutions to Equations 8 to 11.

METHOD OF SOLUTION

The spectral-homotopy analysis method is applied to solve the system of differential Equations 8 to 11 subject to the boundary conditions (Equation 13). We first use the domain truncation method to approximate the domain of the problem from $[0,\infty)$ to $[0,L]$, where L is chosen to be sufficiently large. We then transform $[0,L]$ to the domain $[-1,1]$ on which the Chebyshev spectral method can be applied by using the transformations:

$$x=\frac{2\eta}{L}-1\quad\text{where}\quad x\in[-1,1]. \quad (14)$$

For convenience, we introduce the transformations:

$$F(\eta)=F_0(\eta)+f(x),\quad H(\eta)=H_0(\eta)+h(x), \quad (15)$$

$$G(\eta)=G_0(\eta)+g(x),\quad \theta(\eta)=\theta_0(\eta)+\phi(x). \quad (16)$$

Where:

$$F_0(\eta)=\eta e^{-\eta},\quad H_0(\eta)=H_w e^{-\eta},\quad G_0(\eta)=e^{-\eta},\quad \theta_0(\eta)=e^{-\eta} \quad (17)$$

are initial approximations that are chosen to satisfy the boundary conditions. To find the functions f, h, g, and ϕ, we proceed as follows. Substituting Equations 14 to 16 into Equations 8 to 11 gives:

$$f''+a_{11}f'+a_{12}f+a_{13}g+a_{14}h-\frac{L}{2}fh+\frac{L^2}{4}(g^2-f^2)=\Phi_1(\eta), \quad (18)$$

$$h''+a_{21}h'+a_{22}h+a_{23}\phi-\frac{L}{2}hh'=\Phi_2(\eta), \quad (19)$$

$$g''+a_{31}g'+a_{32}g+a_{33}f+a_{34}h-\frac{L}{2}hg'-\frac{1}{2}L^2fg=\Phi_3(\eta), \quad (20)$$

$$\phi''+a_{41}\phi'+a_{42}h'+a_{43}h+a_{44}g'+a_{45}g+a_{46}f'+a_{47}f+L^2PrEc(\frac{1}{Re}+\frac{M}{4})f^2$$

$$+\frac{L^2PrEcM}{4}g^2+PrEc[(f')^2+(g')^2]+\frac{2PrEc}{Re}(h')^2-\frac{LPr}{2}h\phi'=\Phi_4(\eta), \quad (21)$$

subject to the boundary conditions:

$$f(-1)=f(1)=h(-1)=h(1)=g(-1)=g(1)=\phi(-1)=\phi(1)=0, \tag{22}$$

Where:

$$\left.\begin{aligned}
&a_{11}=-\frac{L}{2}H_0,\quad a_{12}=-\frac{L^2}{4}\left(\frac{1}{Da}+\frac{M}{1+s^2}+2F_0\right), a_{13}=\frac{L^2}{4}\left(\frac{Ms}{1+s^2}+2G_0\right)\\
&a_{14}=-\frac{L^2}{4}F_0', a_{21}=-\frac{L}{2}H_0,\qquad a_{22}=\frac{L^2}{4}\left(-\frac{1}{Da}-H_0'\right),\\
&a_{23}=\frac{L^2Gr}{4},\quad a_{31}=-\frac{L}{2}H_0,\qquad a_{32}=-\frac{L^2}{4}\left(\frac{1}{Da}+\frac{M}{1+s^2}+2F_0\right)\\
&a_{33}-=\frac{L^2}{4}\left(2G_0+\frac{Ms}{1+s^2}\right), a_{34}=-\frac{L}{4}G_0',\quad a_{41}=-\frac{L}{2}PrH_0,\\
&a_{42}=\frac{2LPrEcH_0'}{Re},\quad a_{43}=-\frac{L^2Pr\theta_0'}{4},\quad a_{44}=-LPrEcG_0'\\
&a_{45}=\frac{L^2PrEcM}{2},\quad a_{46}=LPrEcF_0',\quad a_{47}=\frac{L^2PrEc}{2}\left(\frac{4EcF_0}{Re}+MF_0\right)
\end{aligned}\right\} \tag{23}$$

The primes in Equations 18 to 21 now denote differentiation with respect to x and

$$\left.\begin{aligned}
&\Phi_1(\eta)=\frac{L^2}{4}\left(F_0'H_0+\frac{1}{Da}F_0+F_0^2+\frac{M}{1+s^2}F_0-F_0''-\frac{Ms}{1+s^2}G_0-G_0^2\right)\\
&\Phi_2(\eta)=\frac{L^2}{4}\left(H_0H_0'+\frac{H_0}{Da}-H_0''-G_r\theta_0\right)\\
&\Phi_3(\eta)=\frac{L^2}{4}\left(H_0G_0'+\frac{1}{Da}+\frac{M}{1+s^2}G_0+\frac{Ms}{1+s^2}F_0+2F_0G_0-G_0''\right)\\
&\Phi_4(\eta)=\frac{PrEcL^2}{4}\left(\frac{H_0\theta_0'}{Ec}-\frac{2(H_0')^2+4F_0^2}{Re}-\theta_0''-(G_0')^2-MG_0^2-(F_0')^2-MF_0^2\right)
\end{aligned}\right\} \tag{24}$$

We select the linear operators:

$$L[F(x;q),H(x;q),G(x;q),\theta(x;q)]=$$

$$\begin{bmatrix}
\dfrac{\partial^2F}{\partial x^2}+a_{11}\dfrac{\partial F}{\partial x}+a_{12}F+a_{13}G+a_{14}\dfrac{\partial H}{\partial x}\\
\dfrac{\partial^2H}{\partial x^2}+a_{12}\dfrac{\partial H}{\partial x}+a_{22}H+a_{23}\theta\\
\dfrac{\partial^2G}{\partial x^2}+a_{31}\dfrac{\partial G}{\partial x}+a_{32}G+a_{33}F+a_{34}H\\
\dfrac{\partial^2\theta}{\partial x^2}+a_{41}\dfrac{\partial\theta}{\partial x}+a_{42}\dfrac{\partial H}{\partial x}+a_{43}H+a_{44}\dfrac{\partial G}{\partial x}+a_{45}G+a_{46}\dfrac{\partial F}{\partial x}+a_{47}F
\end{bmatrix}$$

where $q\in(0,1)$ is the embedding parameter. We also demand that the initial approximations be the solutions of the linear equations:

$$f_0''+a_{11}f_0'+a_{12}f_0+a_{13}g_0+a_{14}h_0=\Phi_1(\eta), \tag{25}$$

$$h_0''+a_{21}h_0'+a_{22}h_0+a_{23}\phi_0=\Phi_2(\eta), \tag{26}$$

$$g_0''+a_{31}g_0'+a_{32}g_0+a_{33}f_0+a_{34}h_0=\Phi_3(\eta), \tag{27}$$

$$\phi_0''+a_{41}\phi_0'+a_{42}h_0'+a_{43}h_0+a_{44}g_0'+a_{45}g_0+a_{45}f_0'+a_{47}f_0=\Phi_4(\eta), \tag{28}$$

subject to the boundary conditions:

$$f_0(-1)=f_0(1)=h_0(-1)=h_0(1)=g_0(-1)=g_0(1)=\phi_0(-1)=\phi_0(1)=0. \tag{29}$$

Equations 25 to 28 are to be solved, subject to the boundary conditions (Equation 29). If an exact solution cannot be found, we use the Chebyshev pseudospectral method to solve the equations. The derivatives of the functions $f_i(x)$, $h_i(x)$, $g_i(x)$, and $\phi_i(x)$ at the collocation points x_j are given by:

$$\left.\begin{aligned}
&\frac{df_i(x_j)}{dx}=\sum_{k=0}^{N}D_{kj}f_i(x_j),\quad \frac{d^2f_i(x_j)}{dx^2}=\sum_{k=0}^{N}D_{kj}^2f_i(x_j)\\
&\frac{dh_i(x_j)}{dx}=\sum_{k=0}^{N}D_{kj}h_i(x_j),\quad \frac{d^2h_i(x_j)}{dx^2}=\sum_{k=0}^{N}D_{kj}^2h_i(x_j)\\
&\frac{dg_i(x_j)}{dx}=\sum_{k=0}^{N}D_{kj}g_i(x_j),\quad \frac{d^2g_i(x_j)}{dx^2}=\sum_{k=0}^{N}D_{kj}^2g_i(x_j)\\
&\frac{d\phi_i(x_j)}{dx}=\sum_{k=0}^{N}D_{kj}\phi_i(x_j),\quad \frac{d^2\phi_i(x_j)}{dx^2}=\sum_{k=0}^{N}D_{kj}^2\phi_i(x_j)
\end{aligned}\right\} \tag{30}$$

The collocation points x_j are given by:

$$x_j=\cos\frac{\pi j}{N},\qquad j=0,1,2,...,N. \tag{31}$$

and D is the Chebyshev spectral differentiation matrix whose entries (Canuto et al., 1988; Trefethen, 2000) are:

$$\left.\begin{aligned}
&D_{kj}=-\frac{1}{2}\frac{c_k}{c_j}\frac{(-1)^{k+j}}{\sin\frac{\pi}{2N}(j+k)\sin\frac{\pi}{2N}(j-k)},\quad j\neq k\\
&D_{kj}=-\frac{1}{2}\frac{\cos\frac{\pi k}{N}}{\sin^2\frac{\pi k}{N}},\qquad k\neq 0\\
&D_{00}=-D_{NN}=\frac{2N^2+1}{6}\\
&D_{kj}=-D_{N-k,N-j},\quad k=\frac{N}{2}+1,\ldots,N.
\end{aligned}\right\} \tag{32}$$

Here, $c_0=c_N=2$ and $c_j=1$ with $1\le j\le N-1$.

Substituting Equations 30 and 31 in 25 to 28 gives a system of equations of the form:

$$AY=B \tag{33}$$

where matrix A has dimensions $4(N+1)\times 4(N+1)$, while matrices B and Y have dimensions $4(N+1)\times 1$.

The zeroth deformation equation is given by:

$$\begin{aligned}
&(1-q)L\{F(x;q),H(x;q),G(x;q),\theta(x;q)\}-[f_0(x),h_0(x),g_0(x),\phi_0(x)]\\
&=q\hbar\{N[F(x;q),H(x;q),G(x;q),\theta(x;q)]-B\}
\end{aligned} \tag{34}$$

where N is the nonlinear differential operator:

$$N[F(x;q),H(x;q),G(x;q),\theta(x;q)]=\begin{bmatrix}
N_1[F(x;q),H(x;q),G(x;q),\theta(x;q)]\\
N_2[F(x;q),H(x;q),G(x;q),\theta(x;q)]\\
N_3[F(x;q),H(x;q),G(x;q),\theta(x;q)]\\
N_4[F(x;q),H(x;q),G(x;q),\theta(x;q)]
\end{bmatrix} \tag{35}$$

with

$$N_1[F(x;q),H(x;q),G(x;q),\theta(x;q)] = \frac{\partial^2 F}{\partial x^2} + a_{11}\frac{\partial F}{\partial x} + a_{12}F + a_{13}G + a_{24}H - \frac{L}{2}H\frac{\partial F}{\partial x} - \frac{L^2}{4}F^2 + \frac{L^2}{4}G^2 \quad (36)$$

$$N_2[F(x;q),H(x;q),G(x;q),\theta(x;q)] = \frac{\partial^2 H}{\partial x^2} + a_{12}\frac{\partial H}{\partial x} + a_{22}H + a_{23}\theta - \frac{L}{2}H\frac{\partial H}{\partial x} \quad (37)$$

$$N_3[F(x;q),H(x;q),G(x;q),\theta(x;q)] = \frac{\partial^2 G}{\partial x^2} + a_{31}\frac{\partial G}{\partial x} + a_{32}G + a_{33}F + a_{34}H - \frac{L}{2}H\frac{\partial G}{\partial x} - \frac{1}{2}L^2FG \quad (38)$$

$$N_4[F(x;q),H(x;q),G(x;q),\theta(x;q)] = \frac{\partial^2 \theta}{\partial x^2} + a_{41}\frac{\partial \theta}{\partial x} + a_{42}\frac{\partial H}{\partial x} + a_{43}H + a_{44}\frac{\partial G}{\partial x} + a_{45}G + a_{46}\frac{\partial F}{\partial x} + a_{47}F + \frac{L^2PrEcM}{4}G^2 + L^2PrEc\left(\frac{1}{Re}+\frac{M}{4}\right)F^2 + PrEc\left(\frac{\partial F}{\partial x}\right)^2 + PrEc\left(\frac{\partial G}{\partial x}\right)^2 + \frac{2PrEc}{Re}\left(\frac{\partial H}{\partial x}\right)^2 - \frac{LPr}{2}H\frac{\partial \theta}{\partial x} \quad (39)$$

The m th order deformation equations are given by:

$$L\{[f_m(x),h_m(x),g_m(x),\phi_m(x)] - \chi[f_{m-1}(x),h_{m-1}(x),g_{m-1}(x),\phi_{m-1}(x)]\} = \hbar R_m \quad (40)$$

where

$$\chi_m = \begin{cases} 0, & m \le 1 \\ 1, & m > 1 \end{cases} \quad (41)$$

subject to boundary conditions:

$$f_m(-1) = f_m(1) = h_m(-1) = h_m(1) = g_m(-1) = g_m(1) = \phi_m(-1) = \phi_m(1) = 0 \quad (42)$$

where

$$R_m = \begin{bmatrix} R_{m,1}(x) \\ R_{m,2}(x) \\ R_{m,3}(x) \\ R_{m,4}(x) \end{bmatrix} \quad (43)$$

with

$$R_{m,1}(x) = f'''_{m-1} + a_{11}f''_{m-1} + a_{12}f'_{m-1} + a_{13}g_{m-1} + a_{14}h_{m-1} - \Phi_1(\eta)(1-\chi_m) - \frac{1}{2}L\sum_{n=0}^{m-1}f''_n h_{m-1-n} + \frac{1}{4}L^2\sum_{n=0}^{m-1}(g_n g_{m-1-n} - f_n f_{m-1-n}) \quad (44)$$

$$R_{m,2}(x) = h''_{m-1} + a_{21}h'_{m-1} + a_{22}h_{m-1} + a_{23}\phi_{m-1} - \Phi_2(\eta)(1-\chi_m) - \frac{1}{2}L\sum_{n=0}^{m-1}h_n h'_{m-1-n} \quad (45)$$

$$R_{m,3}(x) = g''_{m-1} + a_{31}g'_{m-1} + a_{32}g_{m-1} + a_{33}f_{m-1} + a_{34}h_{m-1} - \Phi_3(\eta)(1-\chi_m) - \frac{1}{2}L\sum_{n=0}^{m-1}h_n g'_{m-1-n} - \frac{1}{2}L^2\sum_{n=0}^{m-1}f_n g_{m-1-n} \quad (46)$$

$$R_{m,4}(x) = \phi''_{m-1} + a_{41}\phi'_{m-1} + a_{42}h'_{m-1} + a_{43}h_{m-1} + a_{44}g'_{m-1} + a_{45}g_{m-1} + a_{46}f'_{m-1} + a_{47}f_{m-1} - \Phi_4(\eta)(1-\chi_m) + L^2PrEr\left(\frac{1}{Re}+\frac{M}{4}\right)\sum_{n=0}^{m-1}f_n f_{m-1-n} + \frac{1}{4}L^2PrEcM\sum_{n=0}^{m-1}g_n g_{m-1-n} + PrEc\sum_{n=0}^{m-1}\left(f''_n f'_{m-1-n} + g'_n g'_{m-1-n}\right) + \frac{2PrEc}{Re}\sum_{n=0}^{m-1-n}h'_n h'_{m-1-n} - \frac{1}{2}LPr\sum_{n=0}^{m-1}h_n\phi'_{m-1-n} \quad (47)$$

Now we use the Chebyshev pseudospectral transformation on equations (40)-(47) to get:

$$AY_m = (\chi + \hbar)AY_{m-1} - \hbar(1-\chi_m)B + \hbar C_{m-1} \quad (48)$$

subject to the boundary conditions (Equation 42) and

$$Y_m = \begin{bmatrix} f_m \\ h_m \\ g_m \\ \phi_m \end{bmatrix}, \qquad C_{m-1} = \begin{bmatrix} P_{m-1} \\ Q_{m-1} \\ S_{m-1} \\ W_{m-1} \end{bmatrix} \quad (49)$$

and

$$P_{m-1} = -\frac{1}{2}L\sum_{n=0}^{m-1}Df_n h_{m-1-n} + \frac{1}{4}L^2\sum_{n=0}^{m-1}(g_n g_{m-1-n} - f_n f_{m-1-n}) \quad (50)$$

$$Q_{m-1} = -\frac{1}{2}L\sum_{n=0}^{m-1}Dh_n h_{m-1-n} \quad (51)$$

$$S_{m-1} = -\frac{1}{2}L\sum_{n=0}^{m-1}h_n Dg_{m-1-n} - \frac{1}{2}L^2\sum_{n=0}^{m-1}f_n g_{m-1-n} \quad (52)$$

$$W_{m-1} = L^2PrEr\left(\frac{1}{Re}+\frac{M}{4}\right)\sum_{n=0}^{m-1}f_n f_{m-1-n} + \frac{1}{4}L^2PrEcM\sum_{n=0}^{m-1}g_n g_{m-1-n} + PrEc\sum_{n=0}^{m-1}\left(f_n Df_{m-1-n} + Dg_n Dg_{m-1-n}\right) + \frac{2PrEc}{Re}\sum_{n=0}^{m-1-n}Dh_n Dh_{m-1-n} - \frac{1}{2}LPr\sum_{n=0}^{m-1}h_n D\phi_{m-1-n} \quad (53)$$

Then, we obtain the following recursive formula for $m \ge 1$:

$$Y_m = (\chi_m + \hbar)Y_{m-1} + \hbar A^{-1}[C_{m-1} - (1-\chi_m)B] \quad (54)$$

Starting from initial approximation obtained from Equation 33, we can calculate the *m*th order approximations using the iteration formula (Equation 54).

Convergence of SHAM solution

As in the case of the standard homotopy analysis method, the convergence of SHAM depends on a careful selection of the auxiliary parameter $\hbar$ which controls the convergence of the series solutions. The standard way of choosing admissible values of $\hbar$ that ensure convergence of the approximate series solution is to

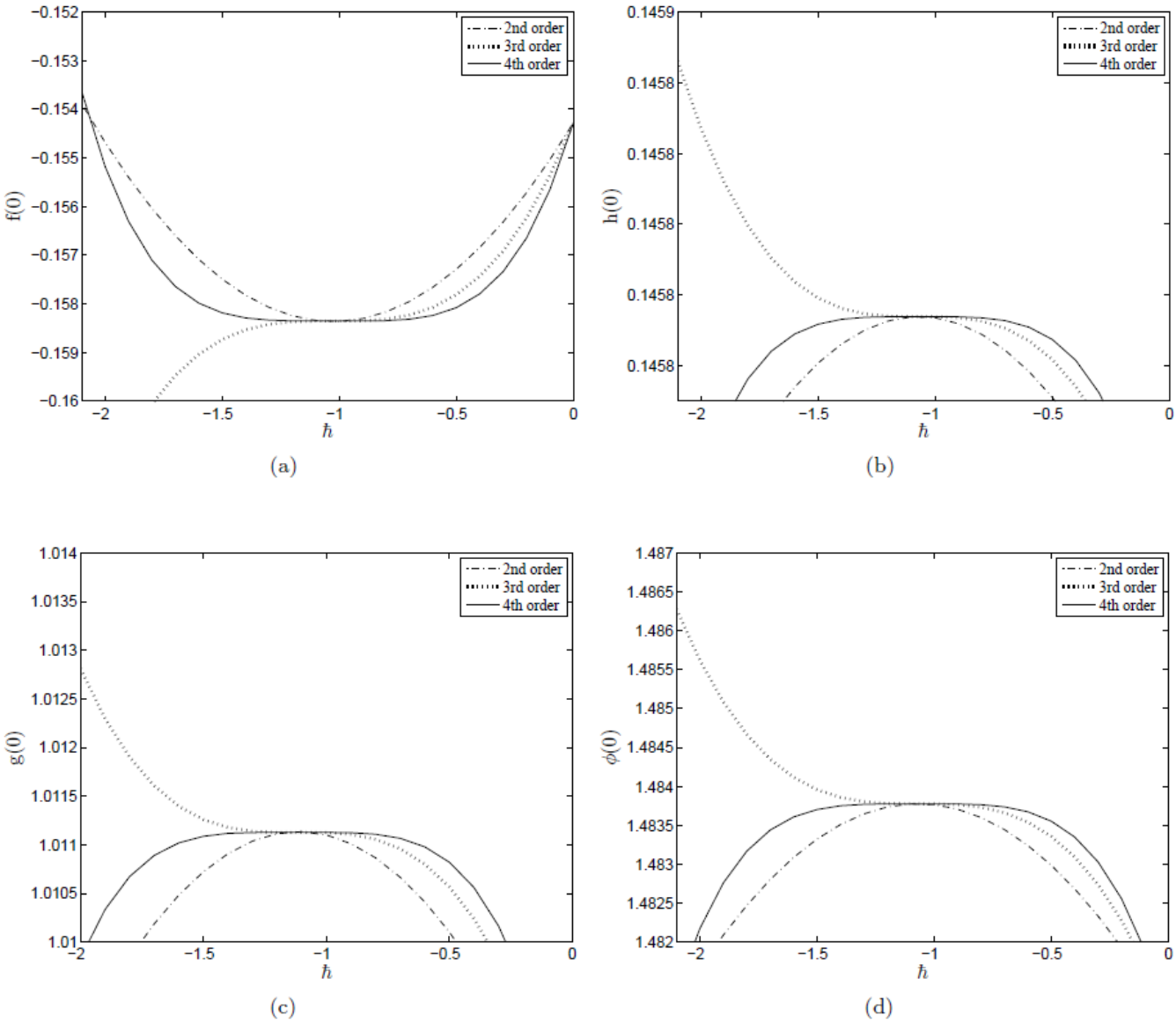

Figure 1. The $\hbar$-curves for the solution series of *F(0)*, *H(0)*, *G(0)*, and -θ*(0)* at 2nd order, 3rd order and 4th order of approximations when *s*=1, *M*=1, *Gr*=0.1, *Pr*=0.71, *Re*=1, *Ec*=0.1, *Da*=1, and *Hw*=0.1.

select a value of $\hbar$ on the horizontal segment of the so-called $\hbar$-curves. Sibanda et al. (2012) suggested that the optimal value of $\hbar$ to use corresponds to the turning point of the second order $\hbar$-curve. In Figures 1, we show the $\hbar$ curves for different orders of SHAM approximation. The optimal value of $\hbar$ that gave the most accurate results is the value at which the maximum or minimum of the second order SHAM $\hbar$-curve is located. We also observe that for higher order approximations, the length of the horizontal segment of the $\hbar$-curve is larger, giving a wider range of valid $\hbar$-values for which the method will converge. The optimum value used in subsequent calculations is $\hbar = -1.1$ at $L = 30$ and $N = 40$. The results below have been generated for $\Pr = 0.71$ and $Gr = 0.1$.

Figures 2 show the convergence of the method solutions for different orders. We note that there is a good convergence to the solutions series starting from the second order approximation.

RESULTS AND DISCUSSION

The effect of the various values parameters M, Da, Ec, and s on the radial and tangential skin frictions and the heat transfer coefficients are given in Table 1. We observe that both the radial and tangential skin friction coefficients increases with increases in M (which is in line with the findings in Sibanda and Makinde (2010), while the heat transfer rate decreases. An increase in s

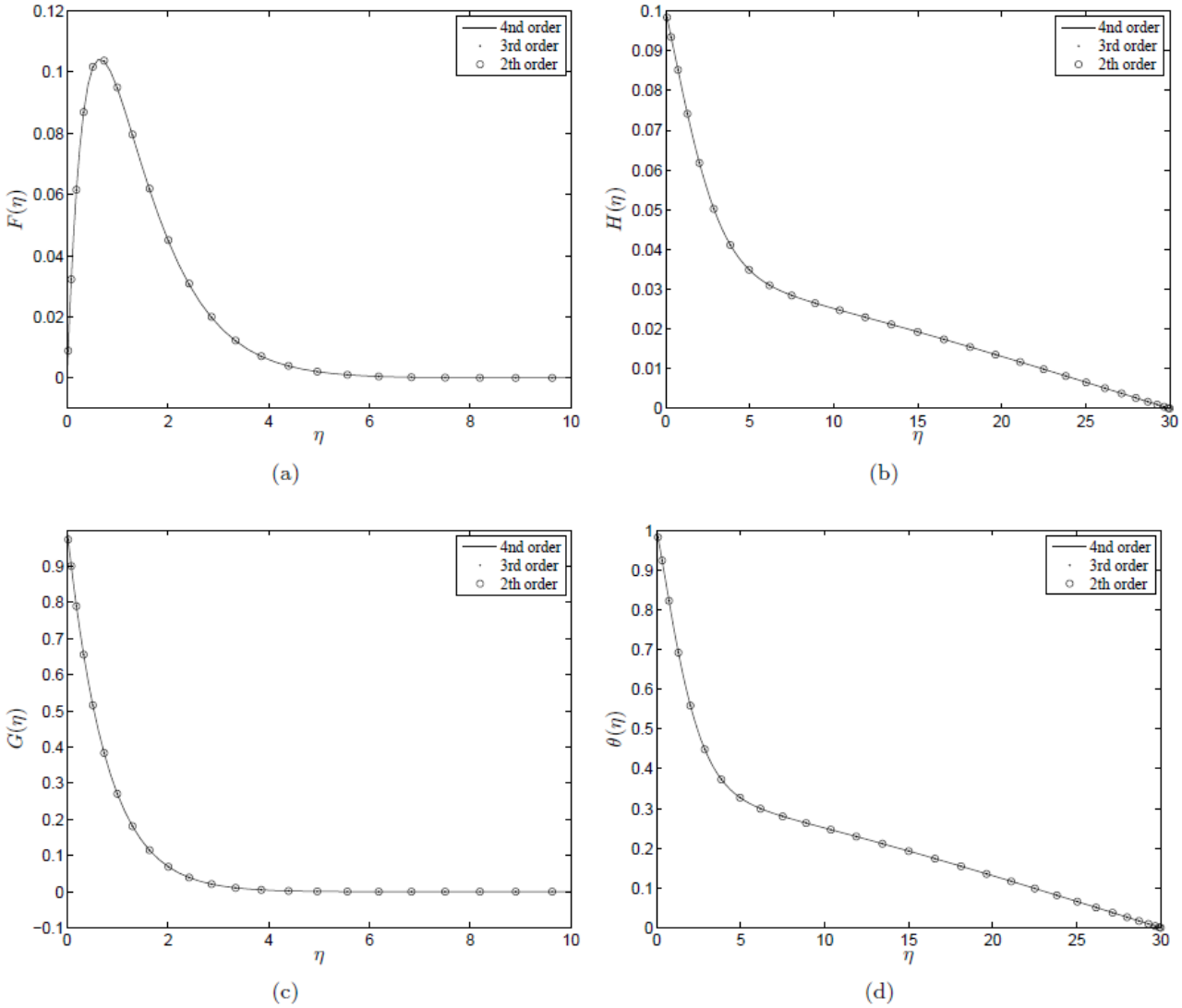

Figure 2. Comparison of the convergence of the SHAM solution of $F(\eta), H(\eta), G(\eta)$ and $\theta(\eta)$ at 2nd order, 3rd order and 4th order of approximations when $\hbar = -1.1, s = 1, M = 1,, Gr = 0.1, Pr = 0.71, Re = 1, Ec = 0.1, Da = 1, and\ H_w = 0.1$.

enhances both the radial skin friction and the rate of heat transfer coefficient while reducing the tangential skin friction. These results are in line with the findings of Osalusi et al. (2007) and Sibanda and Makinde (2010). Furthermore, the radial skin friction increases with increasing Darcy numbers. In Table 1, we notice that as Ec increases, the rate of heat transfer and the radial skin friction increase.

Figure 3 shows the effect of the magnetic interaction parameter M on velocity and temperature profiles when the other parameters are held constant. The results show that the radial velocity achieves a maximum within the boundary layer. The radial, axial, tangential, and the temperature profiles decrease with increasing magnetic field parameters. These findings are in line with the findings in Osalusi et al. (2007) and Sibanda and Makinde (2010).

Figure 4 shows the effects of the Hall current parameter s on the radial and the axial velocity components when all other parameters were held constant. We note that both the radial and the axial velocity components decrease with the Hall current parameter. Back flow in the radial direction is observed for negative values of the Hall parameter.

The effect of fluid suction or injection on the radial and axial velocity components is as shown in Figure 5, it is shown that flow reversal is possible for negative values of s and back flow in the radial direction is observed for suction negative values (Sibanda and Makinde, 2010; Attia and Aboul-Hassan, 2004).

Table 1. Numerical values of F'(0), -G'(0), and -θ'(0) for various values of M, Da, Ec, and s with Gr=0.1, Pr=0.71, Re=1, and Hw-0.1.

M	*Da*	*Ec*	*s*	*F'(0)*	*-G'(0)*	*-θ'(0)*
0.5	1.0	1.0	0.60	0.38193992	1.15609096	1.25432699
1.0	1.0	1.0	0.60	0.44200996	1.27438802	1.14142328
1.5	1.0	1.0	0.60	0.49551577	1.38289745	1.02258803
2.0	1.0	1.0	0.60	0.54417681	1.48370053	0.90106264
1.0	1.5	1.0	0.10	0.49359166	1.13938449	0.19921691
1.0	2.0	1.0	0.10	0.52127588	1.07586299	0.16932975
1.0	3.0	1.0	0.10	0.55365292	1.00937000	0.12482465
1.0	5.0	1.0	0.10	0.58555160	0.94812814	0.00650942
1.0	1.0	1.0	0.40	0.44416242	1.27100369	0.95906528
1.0	1.0	1.0	0.45	0.44349154	1.27273594	1.07018270
1.0	1.0	1.0	0.50	0.44286507	1.27417329	1.15914434
1.0	1.0	1.0	0.55	0.44233745	1.27495095	1.19939908
1.0	1.0	0.1	0.60	0.26364221	1.40317393	1.05024492
1.0	1.0	0.2	0.60	0.29651926	1.40022055	1.07234583
1.0	1.0	0.3	0.60	0.32712875	1.39202391	1.09041404
1.0	1.0	0.4	0.60	0.35447826	1.37960554	1.10477955

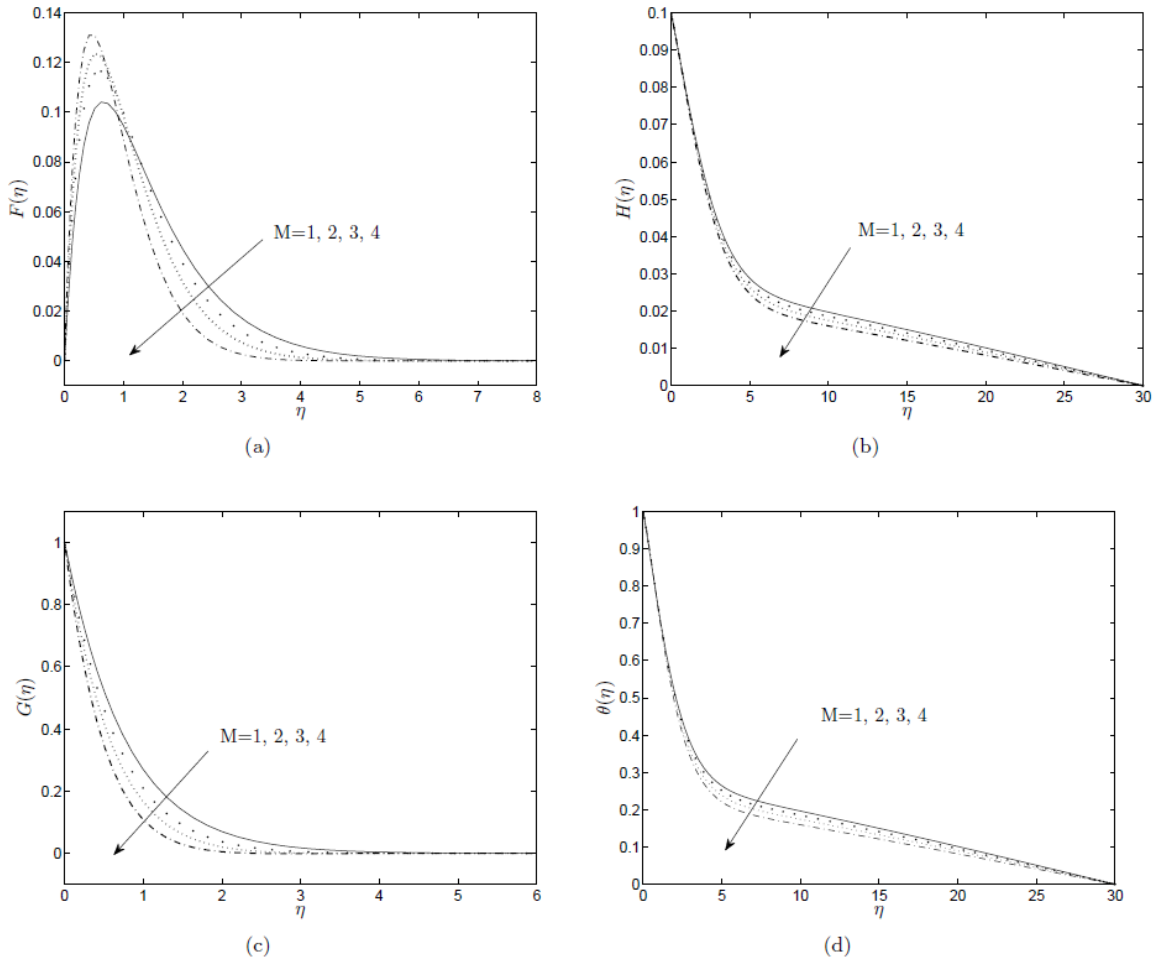

Figure 3. The effect of magnetic field variation on (a) radial, (b) axial (c) tangential velocity components and (d) temperature profile when *s*=1 $s = 1,, Gr = 0.1, Pr = 0.71, Re = 1, Ec = 0.1, Da = 1, and\ H_w = 0.1$ at the 6th order SHAM approximation.

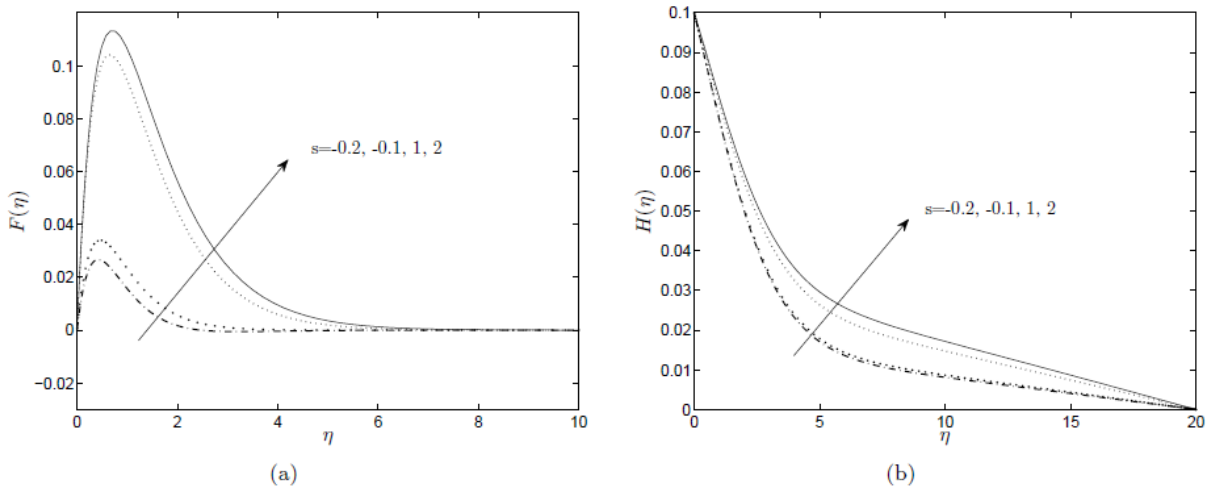

Figure 4. The effect of Hall current variation on (a) the radial and (b) the axial velocity components when M=1, $M = 1,, Gr = 0.1, Pr = 0.71, Re = 1, Ec = 0.1, Da = 1, and\ H_w = 0.1$ at the 6th order SHAM approximation.

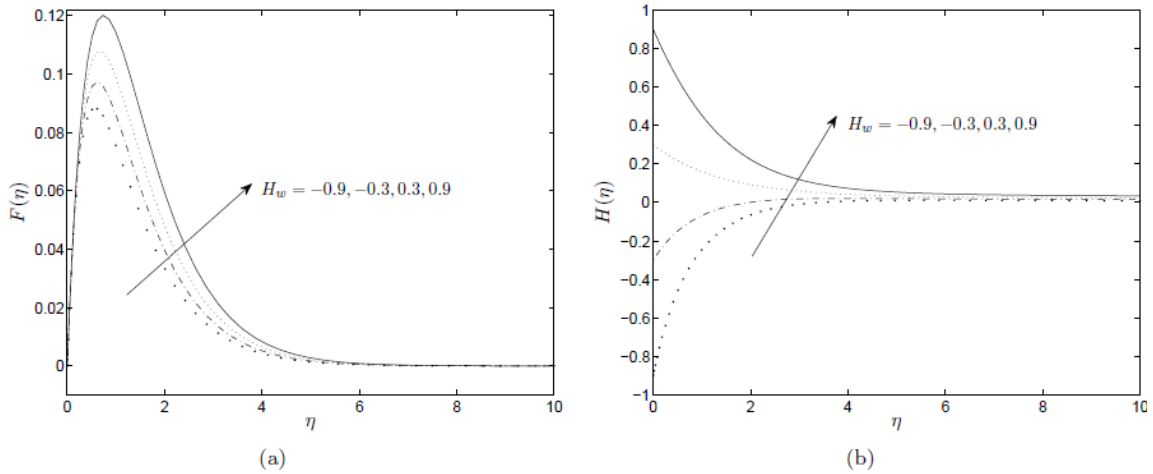

Figure 5. The effect H_W variation on (a) the radial and (b) the axial velocity components when *M*=1, $M = 1,, Gr = 0.1, Pr = 0.71, Re = 1, Ec = 0.1, Da = 1, and\ s = 1$ at the 6th order SHAM approximation.

The effect of increasing the Darcy number Da is to enhance both the boundary-layer velocity and the temperature distribution (Figure 6). Figures 7 illustrates the effect of the Eckert number Ec on axial and tangential velocity components.

Conclusion

In this work, we investigated the steady MHD flow of a viscous incompressible and electrically conducting fluid past a rotating disk in porous medium. A similarity transformation reduced the governing partial differential equations into ordinary differential equations which were then solved using the spectral-homotopy analysis method. SHAM transforms the solution of differential equations to that of a system of algebraic equations which are easier to solve as compared to the differential equations obtained when using the standard HAM. We found high convergence of the series solution for the second order, and we have shown that SHAM gives good accuracy and is computationally efficient.

The results indicate that an increases in the magnetic parameter reduces the radial, axial, tangential, and the temperature profiles. They further show that the effect of the Hall current parameter is to reduce the radial and the axial velocity components. Increasing suction or injection reduces the radial and axial velocity components with

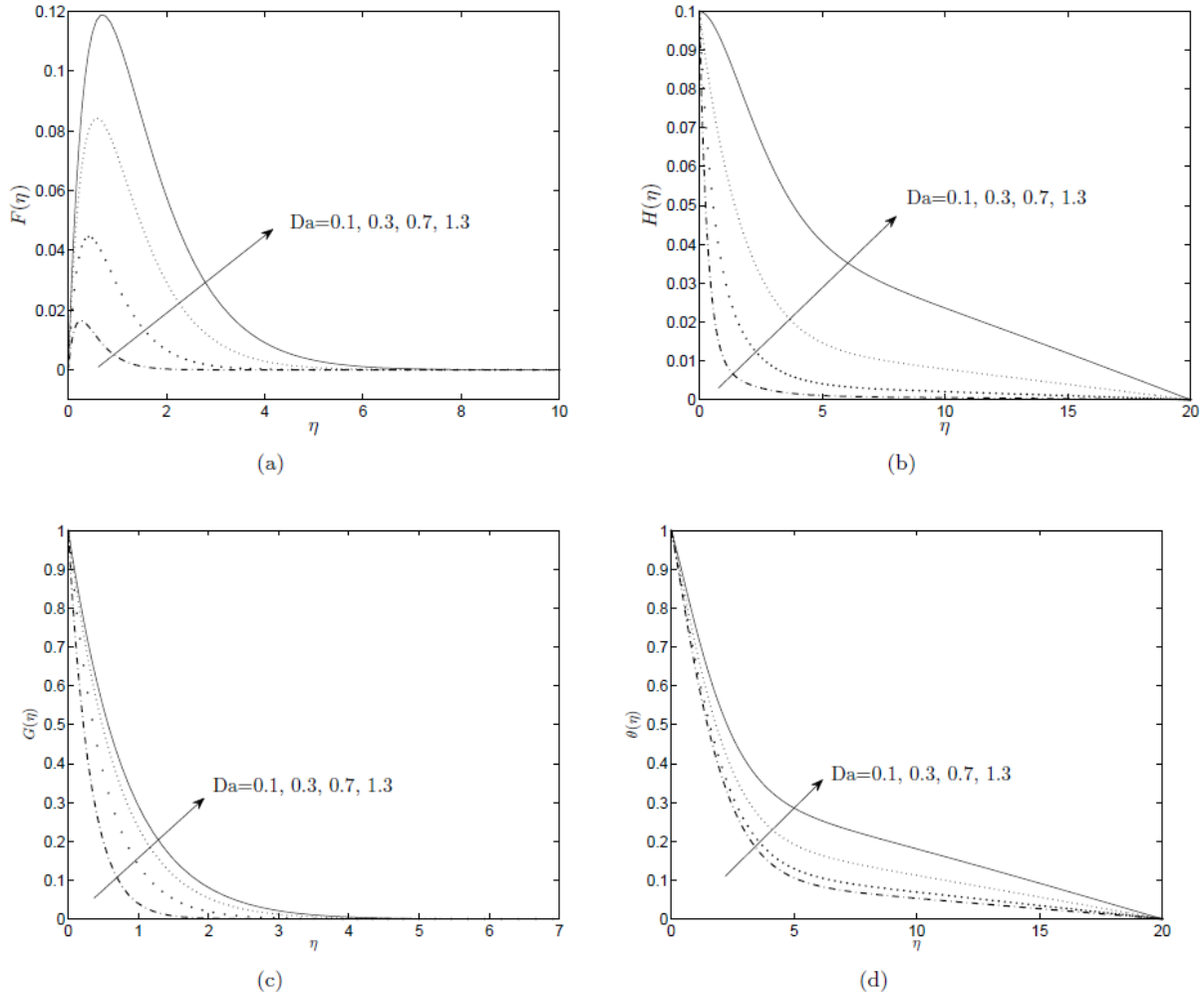

Figure 6. The effect of Darcy number variation on (a) radial, (b) axial (c) tangential velocity components, and (d) temperature profile when $s = 1, M = 1, Gr = 0.1, Pr = 0.71, Re = 1, Ec = 0.1$ *and* $H_w = 0.1$ at the 6th order SHAM approximation.

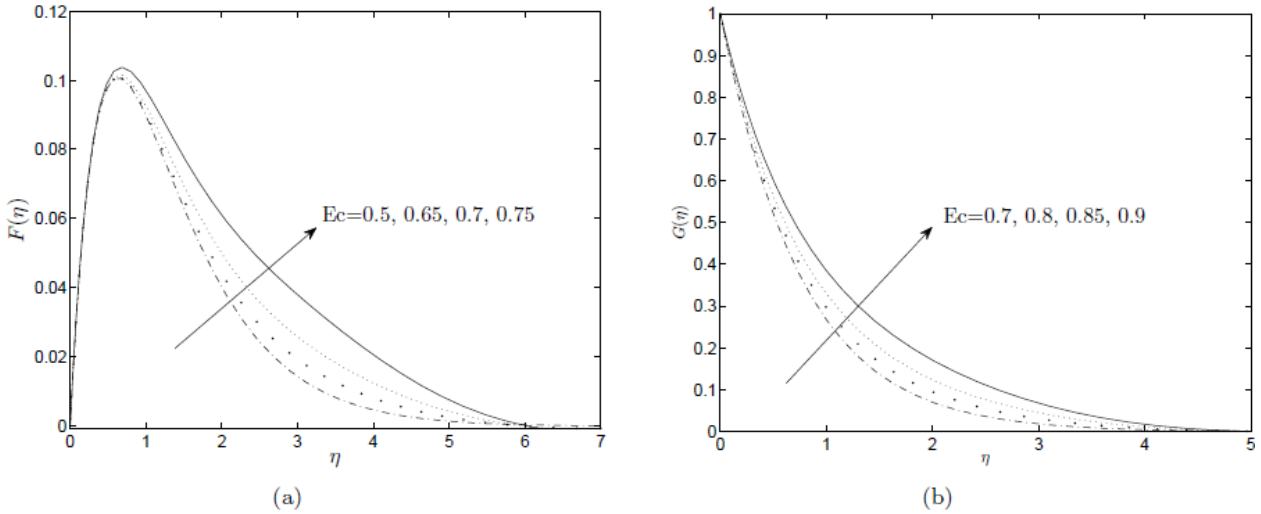

Figure 7. The effect of Eckert number variation on (a) radial and (b) tangential velocity components when $s = 1, M = 1, , Gr = 0.1, Pr = 0.71, Re = 1, Da = 1,$ *and* $H_w = 0.1$ at the 6th order SHAM approximation.

back flow in the radial direction realized for suction negative values. We also showed that the friction coefficient, the magnetic interaction parameter, the Hall parameter, and the Eckert number all combine to increase the skin friction, while increasing the Darcy number reduces the skin friction thereby increasing the fluid velocity"

REFERENCES

Ariel PD (2009). The homotopy perturbation method and analytical solution of theproblem of flow past a rotating disk. Comput. Math. Appl. 58:2504-2513.

Attia HA (2004). Ion slip effect on the flow due to a rotating disk. Arab J. Sci. Eng. 29:165-172.

Attia HA, Aboul-Hassan AL (2004). O Attia n hydromagnetic flow due to a rotating disk, Appl. Math. Modelling 28:1007-1014.

Attia HA (2006). Unsteady flow and heat transfer of viscous incompressible fluid with temperature-dependt viscosity due to the rotating disk in porous medium. J. Phys. A: Math. Gen. 39:979-991.

Attia HA (2007). Rotating disk flow and heat transfer of conducting non-Netonian fluid with suction-injection and ohmic heting. J. Braz. Soc. Mech. Sci. Eng. 19:168-173.

Benton ER (1966). On the flow due to a rotating disk. J. Fluid Mech. 24:781-800.

Canuto C, Hussaini MY, Quarteroni A, Zang TA (1988). Spectral Methods in Fluid Dynamics. Springer-Verlag, Berlin.

Chen CH (2004). Combined heat and mass transfer in MHD free convection from a vertical surface with Ohmic heating and viscous dissipation. Int. J. Eng. Sci. 42:699-713.

Cochran WG (1934). The flow due to a rotating disk. P. Camb. Philos. Soc. 30:365-375.

Dinarvand S, Doosthoseini A, Doosthoseini E, Rashidi MM (2010). Series solutions for unsteady laminar MHD flow near forward stagnation point of an impulsively rotating and translating sphere in presence of buoyancy forces. Nonlinear Analysis: Real World Appl. 11:1159-1169.

Eldabe NT, Ouaf MEM (2006). Chebyshev finite difference method for heat and mass transfer in a hydromagnetic flow of a micropolar fluid past a stretching surface with Ohmic heating and viscous dissipation. Appl. Math. Comput. 177:561-571.

Frusteri F, Osalusi E (2007). On MHD and slip flow over a rotating porous disk with variable properties. Int. Comm. Heat Mass Transf. 34:492-501.

Liao SJ (2005). Comparison between the homotopy analysis method and homotopy perturbation method. Appl. Math. Comput. 169:1186-1194.

Motsa SS, Sibanda P, Awad FG, Shateyi S (2010a). A new spectral-homotopy analysis method for the MHD Jeffery-Hamel problem. Comput. Fluids 39:1219-1225.

Motsa SS, Sibanda P, Shateyi S (2010b). A new spectral-homotopy analysis method for solving a nonlinear second order BVP. Commun. Nonlinear Sci. Numer. Simul. 15:2293-2302.

Osalusi E, Sibanda P (2006). On variable laminar convective flow properties due to a porous rotaing disk in a magnetic field. Rom. J. Phys. 9-10:933-944.

Osalusi E, Side J, Harris R (2007). The effects of Ohmic heating and viscous dissipation on unsteady MHD and slip flow over a porous rotating disk with variable properties in the presence of Hall and ion-slip currents. Int. Comm. Heat Mass Transf. 34:1017-1029.

Osalusi E, Side J, Harris R, Clark P (2008). The effect of combined viscous dissipation and Joule heating on unsteady mixed convection MHD flow on a rotating cone in a rotating fluid with variable properties in the presence of Hall and ion-slip currents. Int. Commun. Heat Mass Transf. 35:413-429.

Rashidi MM, Dinarvand S (2009). Purely analytic approximate solutions for steady three-dimensional problem of condensation film on inclined rotating disk by homotopy analysis method. Nonlinear Analysis: Real World Appl. 10:2346-2356.

Sahoo B (2009). Effects of partial slip, viscous dissipation and Joule heating on Von Karman flow and heat transfer of an electrically conducting non-Newtonian fluid. Commun. Nonlinear Sci. Numer. Simulat. 14:2982-2998.

Sibanda P, Makinde OD (2010). On MHD flow and heat transfer past a rotating disk in porous medium with Ohmic heating and viscous dissipation, Int. J. Numer. Methods Heat Fluid Flow 20:269-285.

Sibanda P, Motsa SS, Makukula ZG (2012). A spectral-homotopy analysis method for heat transfer flow of a third grade fluid between parallel plates. Int. J. Numerical Methods Heat Fluid Flow 22:4-23.

Trefethen LN (2000). Spectral Methods in MATLAB, SIAM.

Turkyilmazoglu M (2009). Purely analytic solutions of the compressible boundary layer flow due to a porous rotating disk with heat transfer. Phys. Fluids 21:106104-12.

Turkyilmazoglu M (2010). The MHD boundary layer flow due to a rough rotating disk. ZAMM Z. Angew. Math. Mech. 90:72–82.

Von Karman T (1921). Uber laminare und turbulente reibung, ZAMM 1:233-235.

Xu H, Liao SJ (2006). Series solutions of unsteady MHD flows above a rotating disk. Meccanica 41:599-609.